

Cellular Interaction of Different Forms of Aluminum Nanoparticles in Rat Alveolar Macrophages

Andrew J. Wagner,^{†,‡} Charles A. Bleckmann,[†] Richard C. Murdock,[‡] Amanda M. Schrand,[‡] John J. Schlager,[‡] and Saber M. Hussain^{*,‡}

Air Force Institute of Technology, Applied Biotechnology Branch, Human Effectiveness Directorate, Air Force, Research Laboratory, Wright-Patterson AFB, Ohio

Received: December 26, 2006; In Final Form: April 10, 2007

Nanomaterials, with dimensions in the 1–100 nm range, possess numerous potential benefits to society. However, there is little characterization of their effects on biological systems, either within the environment or on human health. The present study examines cellular interaction of aluminum oxide and aluminum nanomaterials, including their effect on cell viability and cell phagocytosis, with reference to particle size and the particle's chemical composition. Experiments were performed to characterize initial in vitro cellular effects of rat alveolar macrophages (NR8383) after exposure to aluminum oxide nanoparticles (Al_2O_3 -NP at 30 and 40 nm) and aluminum metal nanoparticles containing a 2–3 nm oxide coat (Al-NP at 50, 80, and 120 nm). Characterization of the nanomaterials, both as received and in situ, was performed using transmission electron microscopy (TEM), dynamic light scattering (DLS), laser Doppler velocimetry (LDV), and/or CytoViva150 Ultra Resolution Imaging (URI). Particles showed significant agglomeration in cell exposure media using DLS and the URI as compared to primary particle size in TEM. Cell viability assay results indicate a marginal effect on macrophage viability after exposure to Al_2O_3 -NP at doses of 100 $\mu\text{g}/\text{mL}$ for 24 h continuous exposure. Al-NP produced significantly reduced viability after 24 h of continuous exposure with doses from 100 to 250 $\mu\text{g}/\text{mL}$. Cell phagocytotic ability was significantly hindered by exposure to 50, 80, or 120 nm Al-NP at 25 $\mu\text{g}/\text{mL}$ for 24 h, but the same concentration (25 $\mu\text{g}/\text{mL}$) had no significant effect on the cellular viability. However, no significant effect on phagocytosis was observed with Al_2O_3 -NP. In summary, these results show that Al-NP exhibit greater toxicity and more significantly diminish the phagocytotic ability of macrophages after 24 h of exposure when compared to Al_2O_3 -NP.

1. Introduction

Metal nanoparticles and their oxides have a considerable number of present and future applications in the military, medical, and industrial fields, but few studies have looked at the toxicological effects of in vitro exposure to metal nanoparticles. Aluminum nanoparticles have been proposed as drug delivery systems, specifically by encapsulating the drugs with nanosized aluminum to increase solubility, thus avoiding clearance mechanisms and allowing for site-specific targeting of drugs to cells.¹ The Department of Defense (DoD) has used micrometer-sized aluminum particles in energetic systems to increase the specific impulse per weight of composite propellants for possible use in solid rocket fuels. The U.S. Army is also currently experimenting with nanomaterials in solid rocket fuel and researching other military applications of aluminum nanoparticle composites.² Aluminum nanoparticles have been utilized by the U.S. Naval Air Warfare Center to replace lead primers in artillery and wear-resistant coatings on propeller shafts of Naval Mine Countermeasure Ships.^{3,4} In addition, the National Aeronautics and Space Agency (NASA) is currently investigating nanoparticles ranging in size from 20 to 100 nm with a 2–3 nm oxidized coat for an optimal propellant for use in current space shuttle solid-rocket boosters.⁵

However, before these materials are introduced throughout diverse levels of occupations or fully integrated into industry and the military, it is important to characterize the risk of nanoparticle exposure. The major toxicological concern of some manufactured nanomaterials, such as Al, is their highly redox active nature⁶ and their ability to cross the cell and mitochondrial membranes.⁷

Since inhalation is one major route of nanomaterial exposure, previous studies have evaluated how nanomaterials might influence the phagocytotic function in alveolar macrophages (AM). One study by Lundborg et al. in 2001 showed that AM exposed to fine and ultrafine carbon particles at a concentration similar to that in urban areas resulted in high particle concentrations outside the cells and impaired the phagocytic function of the AM.⁸ Moreover, Renwick et al. in 2001 looked at carbon black and titanium oxide in the fine and ultrafine size ranges,⁹ and they found that neither of the compounds was directly toxic to the cells; however, a significant reduction in the ability of macrophages to phagocytize other particles was seen. This decrease in phagocytosis was more prevalent in the ultrafine particles as compared to their macrosized counterparts. Furthermore, Guang et al. in 2005 observed that not only do nanoparticles decrease phagocytosis more than macrosized particles, but some particles made of the same material will affect phagocytosis in AM differently, due to different surface characteristics.¹⁰ In addition, single-walled carbon nanotubes were shown to greatly impair phagocytic function more than

* Author to whom correspondence should be addressed. Tel: 937-904-9517. Fax: 937-904-9610. E-mail: saber.hussain@wpafb.af.mil.

[†] Air Force Institute of Technology.

[‡] Applied Biotechnology Branch.

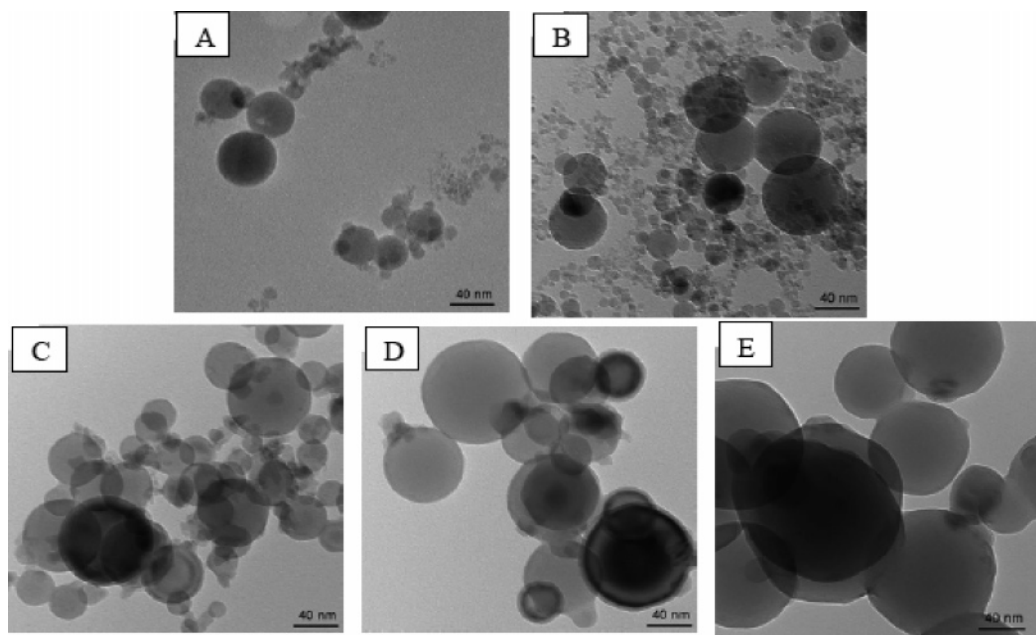


Figure 1. Transmission electron microscopy (TEM) of Al-NP for size comparison. Nanoparticles were observed after suspension in water and subsequent deposition onto formvar/carbon-coated TEM grids as described in Materials and Methods section. Size comparison of measured Al nanoparticle sizes in 1 mg/mL deionized water. (A) Al oxide 30 nm, (B) Al oxide 40 nm, (C) Al 50 nm, (D) Al 80 nm, and (E) Al 120 nm.

TABLE 1: Al Nanoparticle Size Measurements Using TEM^a

particle and size specified by manufacturer	average particle diameter (nm)	standard deviation (nm)
Al ₂ O ₃ 30 nm	48.4	±30.5
Al ₂ O ₃ 40 nm	46.8	±40.0
Al 50 nm	40.2	±17.3
Al 80 nm	67.2	±26.3
Al 120 nm	110	±34.1

^a A total of 100 particles from each size were measured and then statistically evaluated for mean size.

other carbon nanoparticles such as multiwalled carbon nanotubes and fullerenes. Moderate toxicity from aluminum nanoparticles in germ line stem cells has also been shown by Braydich-Stolle et al.¹¹

To our knowledge, no data are currently available on aluminum nanoparticle toxicity in reference to alveolar macrophages. Macrophages are a population of ubiquitously distributed tissue mononuclear phagocytes responsible for numerous homeostatic, immunological, and inflammatory processes. Alveolar macrophages are found in the alveolar sacs deep within the lungs. These cells are the first line of immunological defense against inhaled particles and serve as a good model to investigate how inhaled particles can adversely affect cell function and lead to degradation of health.¹² Therefore, in the present study, immortalized rat alveolar macrophages (NR8383) were selected as a model to assess levels, and explore the mechanisms, of toxicity from aluminum oxide nanoparticles (Al₂O₃-NP) and aluminum nanoparticles (Al-NP). Findings for the general material and cell morphology, cell viability, and phagocytic ability were observed in macrophages following aluminum nanoparticle exposure.

2. Materials and Methods

2.1. Chemicals. The test materials, aluminum oxide nanoparticles (30 nm, 40 nm) and aluminum nanoparticles with a 2–3 nm oxide coat (50 nm, 80 nm, 120 nm), were synthesized

and generously provided by NovaCentrix, Austin, TX. The 3-(4,5-dimethylthiazol-2-yl)-2,5-diphenyltetrazolium bromide (MTT) and Ham's nutrient mixture F-12 media (Kaighn's modified) were received from American Type Culture Collection (ATCC, Manassas, USA). Penicillin/Streptomycin and 2 μm fluorescent latex beads were purchased from Sigma Chemical Company (St. Louis, MO). The nitric oxide kit was obtained from Promega Biosciences Inc. (San Luis Obispo, CA), and enzyme-linked immunosorbant assay (ELISA) cytokine assay kits were purchased from BioSource International Inc. (Camarillo, CA).

2.2. Cell Culture. The rat alveolar macrophages (NR8383 line) were obtained from the American Type Culture Collection (ATCC, Manassas, USA). ATCC describes these cells as homogeneous and highly responsive alveolar macrophages, which can be used in vitro to study macrophage-related activity. The cells were maintained in F12K medium supplemented with 20% fetal bovine serum (FBS) in 1% penicillin and streptomycin. For assays, the cells were seeded in 24-well plates at $\sim 2.5 \times 10^5$ cells/mL (~ 6500 cells/cm²) or 6-well at $\sim 5 \times 10^5$ cells/mL of media (52 000 cells/cm²). Two-chambered slides, used for morphological examination and phagocytosis assays, were seeded at lower concentrations ranging between 1×10^5 and 2.5×10^5 cells/mL. The cells were grown in a humidified incubator at 37 °C and 5% CO₂ atmosphere on a layer of rat tail collagen.

2.3. Nanoparticles and Exposure. Aluminum nanoparticles, received in dry powder form, were suspended in deionized water to make stock solutions (10 mg/mL). Prior to each use, stock solutions were sonicated for 20 s to reduce agglomeration of particles. A range of dilutions were made in cell culture media from stock solutions and mixed by inverting the container 5 times and vortexing for 5 s. Increasing concentrations of nanoparticle suspensions were added to rat alveolar macrophages cultured in 6- and 24-well culture plates or two-chambered slides. For consistency and ease of understanding, nanoparticle concentrations are represented as μg/mL of media throughout the paper.

TABLE 2: Al Nanoparticle Characterization in Solution

particle	DLS		LDV		
	average diameter (nm)	PDI	zeta potential ζ (mV)	electrophoretic mobility μ ($\mu\text{m}\cdot\text{cm}\cdot\text{V}^{-1}\cdot\text{s}^{-1}$)	pH
Al ₂ O ₃ 30 nm					
water	204	0.122	43.2	3.38	7.0
F-12K media with 20% serum	219	0.215			7.5
Al ₂ O ₃ 40 nm					
water	243	0.14	36.4	2.85	7.0
F-12K media with 20% serum	257	0.242			7.5
Al 50 nm					
water	247	0.234	34.4	2.7	7.0
F-12K media with 20% serum	383	0.393			7.5
Al 80 nm					
water	387	0.391	26.1	2.04	7.0
F-12K media with 20% serum	360	0.393			7.5
Al 120 nm					
water	330	0.329	28.0	2.2	7.0
F-12K media with 20% serum	515	0.794			7.5
DI H ₂ O	no reading	N/A			7
F-12K media with 20% serum	15.6 ^b	0.418			7.5

^a Al₂O₃ 30 nm and Al₂O₃ 40 nm samples were measured at 50 $\mu\text{g}/\text{mL}$, whereas the Al 50 nm, Al 80 nm, and Al 120 nm samples were measured at 25 $\mu\text{g}/\text{mL}$. ^b Less than 4% of relative amount in sample volume.

2.4. Agglomeration of Al₂O₃-NP and Al-NP Visualized by Advanced Illuminating Microscopy. Solutions of Al₂O₃-NP and Al-NP were imaged with an Olympus IX71 Microscope platform coupled to the CytoViva 150 Ultra Resolution Imaging (URI) System. A 10 μL aliquot of nanoparticles at different concentrations were evaluated on glass slides with cover slips using the 60 \times oil lens as described in our study by Skebo et al.¹³ QCapture Pro Imaging Software was used to capture and store images.

2.5. Transmission Electron Microscopy (TEM) of Al₂O₃-NP and Al-NP. Transmission electron microscopy (TEM) characterization was performed on a Hitachi H-7600 tungsten-tip instrument at an accelerating voltage of 120 kV. Nanoparticles were examined after suspension in water and subsequent deposition onto Formvar/carbon-coated TEM grids. The AMT software for the digital TEM camera was calibrated for size measurements of the nanoparticles. Mean size was calculated from a random field of view, in addition to images that showed the general morphology of the nanoparticles. Over 100 particles were counted and measured for each nanoparticle size reported.

2.6. Dynamic Light Scattering Analysis (DLS) and Laser Doppler Velocimetry (LDV) of Al₂O₃-NP and Al-NP in Solution. Dynamic light scattering (DLS) and laser Doppler velocimetry (LDV), for characterization of the particles in solution, were performed on a Malvern Instruments Zetasizer Nano ZS instrument. The device uses a 4 mW He-Ne 633 nm laser to analyze the samples as well as an electric field generator (for LDV measurements). Nanoparticles were examined after suspension in water and cell culture/dosing media at concentrations of 25 $\mu\text{g}/\text{mL}$ (Al 80 nm and Al 120 nm) or 50 $\mu\text{g}/\text{mL}$ (Al₂O₃ 30 nm and Al₂O₃ 40 nm). Samples were prepared as dosing solutions, and 1.5 mL was transferred to a square cuvette for DLS measurements or 1 mL was transferred to a Malvern Clear Zeta Potential cell for LDV measurements. Average size was calculated by the software from the intensity, volume, and number distributions measured. The polydispersity index (PDI) given is a measure of the size ranges present in the solution with a scale ranging from 0 to 1, with 0 being monodisperse and 1 being polydisperse.

2.7. Viability Assay. The MTT assay assessed the viability of alveolar macrophages on the basis of mitochondrial function.¹⁴ After 24 h of exposure to different concentrations of

nanoparticles, the media was removed from each well and replaced with MTT solution 10 times, and incubated for approximately 30 min at 37 $^{\circ}\text{C}$ until a purple color developed. The mixture was re-suspended, transferred into eppendorf tubes, and centrifuged for 2 min at 2000g. The supernatant was removed, and 0.5 mL of 70% isopropyl alcohol was added to each dye pellet and vortexed in order to obtain homogeneous staining. Samples (200 μL) were transferred into a 96-well plate, and absorbance was read on a Spectromax 190 spectrophotometer at 570–630 nm. The percent reduction of MTT was compared to the control, which represented 100% MTT reduction. Each dose was done in triplicate for each experiment and repeated at least three times for statistical analysis.

2.8. Phagocytosis Assay. Phagocytosis activity, and its inhibition, for cultured alveolar macrophages following exposure to different nanomaterials, was measured. Alveolar macrophages were seeded on chambered microscope slides at 2.5×10^5 cells/mL media for 2–4 h. The media was then replaced with a nanoparticle solution in media at a concentration of 25 $\mu\text{g}/\text{mL}$ for all sizes of Al-NP (50 nm, 80 nm, 120 nm) and 5 $\mu\text{g}/\text{mL}$ for Al₂O₃-NP (30 nm, 40 nm). These cells were exposed for 24 h to the nanoparticles and then the media was replaced with a solution of 2 μm latex beads in media for 6 h at a 10:1 ratio (10 beads to 1 cell). After 6 h the cells were washed twice with warm media and viewed on an Olympus IX71 inverted fluorescent microscope in conjunction with a high illuminating light source. The microscope and light system allowed for focusing on the cell membrane, nucleus, and latex beads at the same time. This method improved the ability to determine which beads were inside the cells and which were not. A continuous line transect of the slide was viewed, and all cells in each field of view were counted. One hundred cells were counted on each slide, and at least three slides were counted for each nanoparticle exposure at each concentration. A phagocytosis index was determined by multiplying the average number of beads taken up by cells by the percentage of macrophages that were positive (positive cell: any AM that took in at least 1 bead).¹⁵

2.9. Statistical Analysis. All of the experiments were done in triplicate, and the results were presented as mean \pm standard deviation. The experimental data were analyzed by ANOVA using Sigma Stat, where statistical significance was accepted

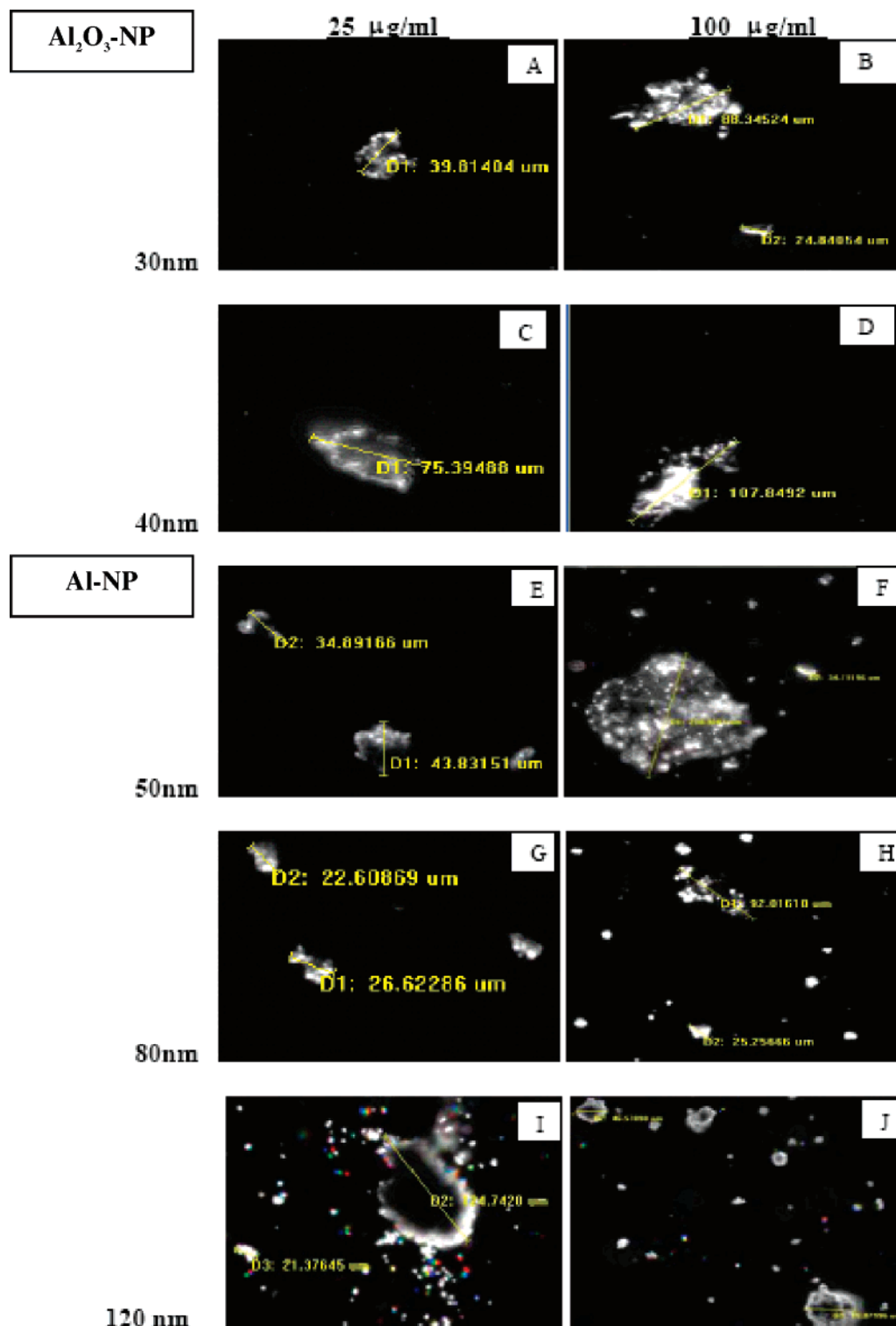


Figure 2. Agglomeration of Al_2O_3 -NP and Al-NP observed by advanced illuminating microscopy. Dispersed agglomerated particles nanoparticles were examined with an Olympus IX71 microscope platform coupled to the CytoViva150 Ultra Resolution Imaging (URI) System (60 \times magnification) as described in Materials and Methods section. QCapture Pro Imaging Software was used to capture and store images. (A) Al_2O_3 30 nm agglomerated particles in 20% FBS media at 25 $\mu\text{g}/\text{mL}$; (B) same as (A) but at 100 $\mu\text{g}/\text{mL}$. (C) Al_2O_3 40 nm agglomerated particles in 20% FBS media at 25 $\mu\text{g}/\text{mL}$; (D) same as (C) but at 100 $\mu\text{g}/\text{mL}$. (E) Al 50 nm agglomerated particles in 20% FBS media at 25 $\mu\text{g}/\text{mL}$; (F) same as (E) but at 100 $\mu\text{g}/\text{mL}$. (G) Al 80 nm agglomerated particles in 20% FBS media at 25 $\mu\text{g}/\text{mL}$; (H) same as (G) but at 100 $\mu\text{g}/\text{mL}$. (I) Al 120 nm agglomerated particles in 20% FBS media at 25 $\mu\text{g}/\text{mL}$; (J) same as (I) but at 100 $\mu\text{g}/\text{mL}$.

at a level of p value < 0.05 . Results annotated with an asterisk on figure bars are significant at $p < 0.05$.

3. Results

3.1. Dispersion, Agglomeration, and Size Verification of Al_2O_3 -NP and Al-NP. TEM images were taken in an attempt

to verify the primary particle sizes and morphologies of individual nanoparticles after introduction into an aqueous system and subsequent air drying before analysis. As seen in Figure 1A–E, all Al-NP and Al_2O_3 -NP were spherical in shape and could readily be measured when sampled at a concentration of 1 mg/mL in deionized water. A comparison of the actual

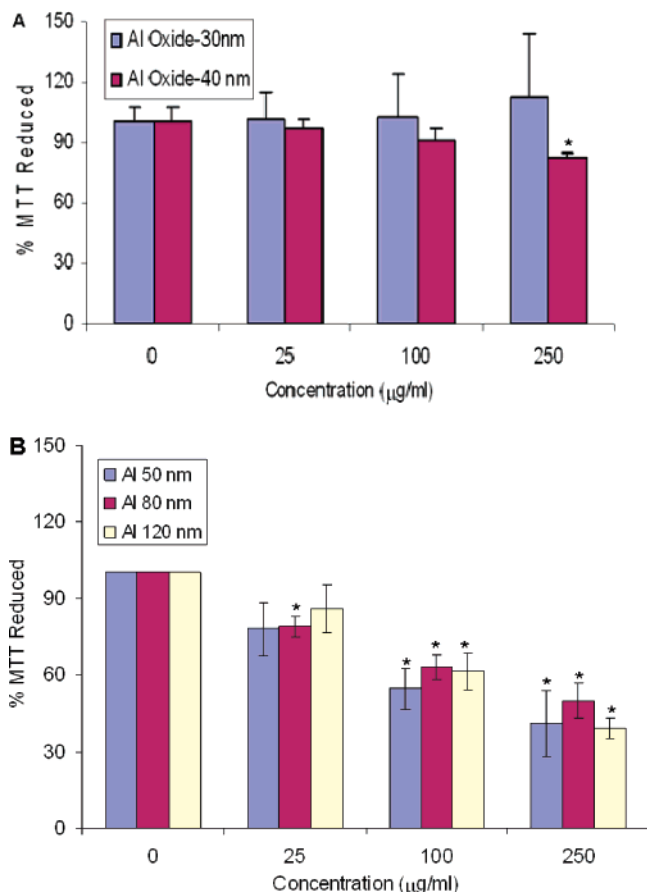


Figure 3. Effect of Al-NP and Al₂O₃-NP on mitochondrial function. Mitochondrial function was determined by the MTT assay as described in Materials and Methods section. Each experimental point is a composite of three independent experiments, with $n \geq 3$ for each point. Statistical significance from control is indicated by the symbol *, where $p < 0.05$. (A) Al-NP (50 nm, 80 nm, and 120 nm) 24 h post exposure, (B) Al₂O₃-NP (30 nm, 40 nm) 24 h post exposure.

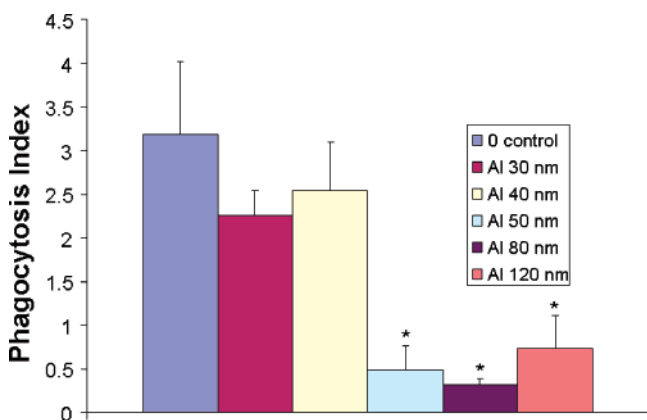


Figure 4. Al₂O₃-NP and Al-NP effect on phagocytosis ability of alveolar macrophages. Phagocytosis Index (P.I.) of alveolar macrophages exposed to various Al nanoparticles at 25 µg/mL for 24 h. P.I. = (% macrophages that take in beads) × (average number of beads taken in by a positive macrophage). The symbol * indicates doses that are significantly different than the zero control, p value < 0.05 .

measured sizes to the manufacturer size estimates is shown in Figure 1A and suggests that the particle size and other characteristics, over a period of time, may change in a dry or aqueous system due to phenomena such as agglomeration. These sizes are not identical, but they are similar to the reported sizes of the manufacturer. However, there is a rather large variance in the mean size of each particle type, as shown by the large

standard deviations in Table 1. This can be explained from the images in Figure 1 where larger particles are found dispersed among much smaller particles. Like agglomeration, size characterization before, during, and once inside the cells needs to be studied further. The size of the nanoparticles throughout the paper are referred to as the sizes specified by the manufacturer in the dry powder form (Al₂O₃ 30 nm, 40 nm, and Al 50 nm, 80 nm, 120 nm). Future studies should assess a greater number of conditions for nanoparticle size measurements and should compare the nanoparticle characteristics in media used during in vitro experiments to nanoparticle characteristics in alveolar fluid found in the lungs.

The DLS results for particle size in solution for the Al nanoparticles are presented in Table 2. As shown by almost all samples measured, the Al particles agglomerated at approximately the same average diameter or larger when dispersed in either water or cell culture media. The Al₂O₃ 30 nm particles agglomerated to average sizes of 204 nm (DI H₂O) and 219 nm (F-12K), while the Al₂O₃ 40 nm particles agglomerated to average sizes of 243 nm and 257 nm. The Al 80 nm and Al 120 nm particles had average sizes of 387 nm/360 nm and 330 nm/515 nm, respectively. The Al₂O₃ 30 nm, 40 nm, and Al 80 nm particles showed less than an 8% change in agglomeration size when dispersed in cell culture media (F-12K) as compared to dispersion in water. The Al 120 nm exhibited a larger change with a 56% increase in average agglomerate diameter. Particles were analyzed in F-12K media with no serum as well, where it was observed that average agglomerate diameter reached as high as 1610 nm. It appears that the proteins in the serum mitigate the agglomeration of the particles in cell culture media close to average sizes measured in water. DI H₂O and F-12K media with 20% serum, both without particles, were analyzed by DLS as negative controls. The DI H₂O samples had particle concentrations below detection limits. The F-12K media with 20% serum sample showed particles present with an average size of 15 nm; however, these particles constituted less than 4% of the sample volume. This 15 nm peak was not observed in samples with the nanoparticles.

LDV results for the measurement of zeta potential and electrophoretic mobility for each particle are also presented in Table 2. The particles dispersed in cell media could not be measured due to the high salt concentrations which corroded the sample chamber electrodes, producing a broad spectrum of zeta potential readings. The Al₂O₃ 30 nm and 40 nm particles, when dispersed in water, were stable suspensions due to their zeta potential being greater than 30 mV (43.2 mV and 36.4 mV). The Al 80 nm and Al 120 nm were very close to this 30 mV (26.1 mV and 28.0 mV) defined line for solution stability. Quantitative stability characterization could not be made; however, a large percentage of the particles should stay suspended with time and little settling would occur.

The agglomerated nanoparticles in situ were observed with the CytoViva150 Ultra Resolution Imaging (URI) system (60× magnification). This analysis was performed to further characterize the dosing solutions, specifically to observe larger (6 µm or greater in diameter) agglomerates of nanoparticles in solution since this is above the range of detection for DLS. This method also allows a quick observation of the state of dispersion for a given solution. Figure 2A,B shows an agglomerate of aluminum oxide nanoparticles in 25 and 100 µg/mL solutions, respectively. The QCapture Pro Imaging software estimated particle size in Figure 2A as approximately 39.8 µm, while in Figure 2B the same particle type, but at a higher concentration (100 µg/mL) had agglomerates of approximately 88.3 µm in size. In compar-

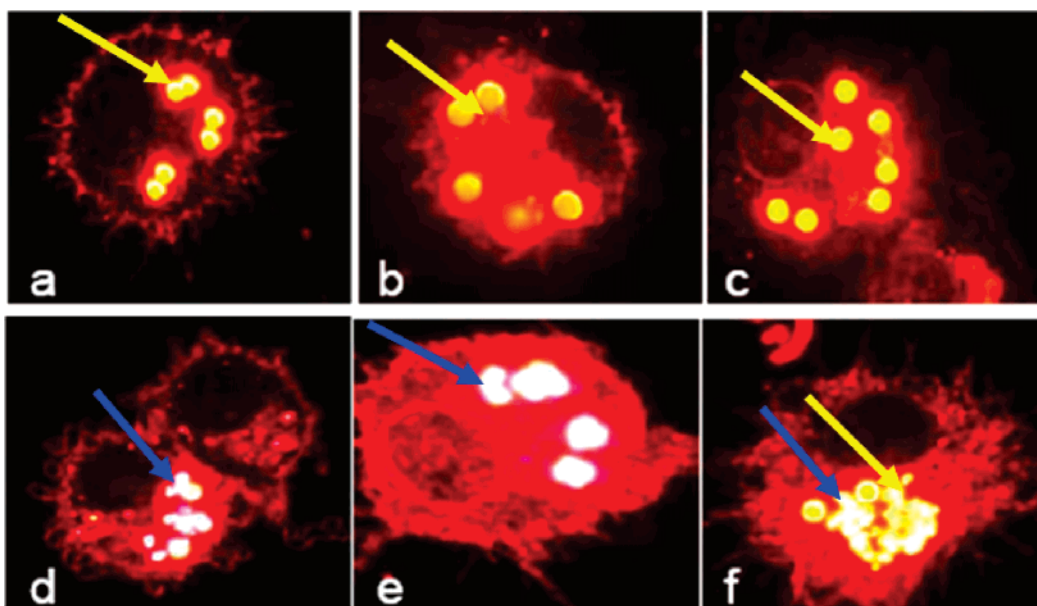


Figure 5. Microscopic observation of Al_2O_3 -NP and Al-NP phagocytosis by alveolar macrophages. Various representative images (a–f) were taken during phagocytosis with the Olympus IX71 inverted fluorescent microscope attached with an advanced high illuminating system. Cells were exposed to Al_2O_3 -NP and Al-NP at 5 or 25 $\mu\text{g}/\text{mL}$ for 24 h. Fluorescent latex beads (2 μm) were given to the cells after exposure. The beads appear as bright globular areas in the cells and were dosed at a 10:1 ratio (10 beads for every cell) for 6 h. Macrophages and beads phagocytized by macrophages were counted to obtain a Phagocytosis Index (P.I.). $\text{P.I.} = (\% \text{ macrophages that take in beads}) \times (\text{average number of beads taken in by a positive macrophage})$. (a) No exposure to Al-NP (control); (b) AM exposed to 25 $\mu\text{g}/\text{mL}$ of Al_2O_3 -NP 30 nm; (c) AM exposed to 25 $\mu\text{g}/\text{mL}$ of Al_2O_3 -NP 40 nm; (d) AM exposed to 5 $\mu\text{g}/\text{mL}$ of Al-NP 50 nm; (e) AM exposed to 5 $\mu\text{g}/\text{mL}$ of Al-NP 80 nm; (f) AM exposed to 5 $\mu\text{g}/\text{mL}$ of Al-NP 120 nm. Yellow arrows indicate uptake of fluorescent latex beads. Blue arrows indicate Al particles uptake.

ing agglomerated particle sizes for Al_2O_3 -NP and Al-NP, size increased with concentration with the exception of Al 120 nm. Figure 2I,J shows that agglomerates at higher concentrations (100 $\mu\text{g}/\text{mL}$) were smaller than those at lower concentration (25 $\mu\text{g}/\text{mL}$). This enhanced agglomeration at smaller primary particle size could be explained by the high surface area/volume ratio of these small particles and that, at higher concentrations, the particles interact more frequently.

3.3. Viability. The MTT assay, a measure of energy-generating potential of the cell and thus overall cell viability, is based upon mitochondrial function. Figure 3A displays the percent of MTT reduction after 24 h of exposure to aluminum nanoparticles (50 nm, 80 nm, 120 nm) showing a significant effect on cell viability. In Figure 3A, Al 50 nm and 120 nm (250 $\mu\text{g}/\text{mL}$) reduced MTT to 40 and 39%, respectively, while at 100 $\mu\text{g}/\text{mL}$, Al 50 nm and 120 nm reduced MTT to 54 and 60%, respectively. Al 80 nm induced a significant reduction of MTT at all three dosing points with 79% at 25 $\mu\text{g}/\text{mL}$, 63% at 100 $\mu\text{g}/\text{mL}$, and 49% at 250 $\mu\text{g}/\text{mL}$.

Results of in vitro exposure of rat alveolar macrophages to Al_2O_3 -NP, with an average size of 30 and 40 nm, are shown in Figure 3B. These results demonstrate that Al_2O_3 -NP 30 nm did not significantly impact the viability of these cells, even at concentrations as high as 250 $\mu\text{g}/\text{mL}$. Also, Al_2O_3 -NP 40 nm at a dose of 250 $\mu\text{g}/\text{mL}$ were significantly different than the controls (p value < 0.05). At 250 $\mu\text{g}/\text{mL}$, 17% of the MTT was reduced when compared to the control. Effects of the 25 $\mu\text{g}/\text{mL}$ Al_2O_3 doses, for both 30 and 40 nm, were not found to be significant (p value > 0.05).

3.4. Phagocytosis Index. The phagocytosis assay was designed to investigate the efficiency of macrophages in assimilating 2 μm latex particles after being exposed to various aluminum nanoparticles for 24 h. Figure 4 indicates that cells dosed with 25 $\mu\text{g}/\text{mL}$ of various Al-NP had a greater reduction in phagocytosis ability than cells dosed with Al_2O_3 -NP. The Al_2O_3 30 nm and Al 40 nm showed a slight, but not significant,

decrease in phagocytosis ability when compared to the control (p value > 0.05). However, Al 50 nm, 80 nm, and 120 nm showed a significant reduction in phagocytosis when compared to the control (p value < 0.05). The control cells had an average phagocytosis index (P.I.) of 3.19, while Al 50 nm, 80 nm, and 120 nm had an average index of 0.49, 0.32, and 0.74, respectively. This represents a 6-, 9-, and 4-fold reduction for each Al-NP. A few representative images of the cells used in the experiment and the fluorescent latex beads they assimilated are seen in Figure 5A–F.

4. Discussion

The purpose of this investigation was to elucidate the potential cytotoxicity of different sizes of aluminum (Al-NP) and aluminum oxide (Al_2O_3 -NP) nanoparticles and to investigate their impact on the phagocytic ability of macrophages. The cytotoxicity was assessed using the MTT assay, while the phagocytic activity of macrophages was assessed by measuring the ability of macrophages to assimilate 2 μm latex beads. Although no toxicity was noted with Al_2O_3 -NP at 24 h exposure, Al-NP displayed a significant decrease in cell viability at 24 h. Furthermore, phagocytic ability of macrophages was significantly impaired following an increased dose of all Al-NP types, while there was no significant effect with Al_2O_3 -NP. The results described in this study provide strong evidence that agglomerated Al-NP and Al_2O_3 -NP were both internalized by the macrophages. The cytotoxicity of the aluminum nanoparticles did not seem to be size- or surface-area-dependent. The distinguishing feature for reducing cell viability and phagocytosis seemed to be the chemical composition of the nanoparticles. It appears that oxide surface coating of the particles prevents aluminum nanoparticles from producing toxicity. Since interactions between nanomaterials and biological organisms typically take place at the particle's surface, the surface characteristics of these materials is of great importance in

determining possible toxic effects. Surface chemistry consists of a wide variety of properties (size, agglomeration state, shape, composition) that govern how particles interact with the biological environment. Recently, Powers et al.¹⁶ addressed and highlighted some of these physicochemical characteristics such as size distribution, shape, chemical composition, particle physicochemical structure, agglomeration state, and concentration, which are essential characteristics that need to be evaluated for toxicological studies. Full characterization of the particles may allow identification of which characteristics induce toxicity. Many of the unique properties of these nanoparticles may significantly affect a variety of cell responses. The dynamics of agglomeration are influenced by the forms of the materials occurring during exposure and producing the effects. Even though the degree of nanoparticle agglomeration in cell media is known, the exact properties of surface characteristics under agglomerated state is not known. Further study is needed to characterize surface properties of these agglomerated particles within the cells to correlate with their toxic properties.

5. Conclusion

As demonstrated by our results, aluminum nanoparticles show chemical-composition-dependent toxicity. The Al-NP were consistently more toxic than the Al₂O₃-NP and had significantly reduced phagocytotic ability. The inhibitory effect on phagocytosis caused by 50 nm, 80 nm, and 120 nm Al-NP at lower nontoxic levels (25 µg/mL) would require further study to determine whether these changes occur in animal models.

Acknowledgment. The authors thank Col. J. Riddle for his strong support and encouragement. We acknowledge Nanoscale Engineering Science and Technology Laboratory (NEST), University of Dayton, for TEM work. Aluminum nanoparticles were generously provided by Dr. Karl Martin at NovaCentrix, Austin, TX. A.S. and R.M. are funded by the Biosciences and Protection Division, Air Force Research Laboratory under Oak Ridge Institute for Science and Education, Oak Ridge, TN. This work was supported by the Air Force Office of Scientific Research (AFOSR) Project (JON # 2312A214).

Supporting Information Available: Limitations and assumptions, visual changes after suspension in media, dynamic light scattering spectra, post exposure effects, and surface area versus MTT assay. This material is available free of charge via the Internet at <http://pubs.acs.org>.

References and Notes

- (1) Tyner, K. M.; Schiffman, S. R.; Giannelis, E. P. Nanobiohybrids as delivery vehicles for camptothecin. *J. Controlled Release* **2004**, *95* (3), 501–514.
- (2) Miziolek, A. Nanoenergetics: An emerging technology area of national importance. *AMPTIAC Q.* **2002**, *6* (1), 43–48.
- (3) Loney, D. (2004) Weapons that Tread Lightly, The Website of the American Chemical Society (2004). 10 January 2006 http://www.chemistry.org/portal/a/c/s/1/feature_ent.html?DOC=enthusiasts%5Cent_greenexplosives.html.
- (4) Department of Defense Director (2005) Defense Research and Engineering, 2005, Defense Nanotechnology Research and Development. 4 January 2006. <http://www.nano.gov/html/res/DefenseNano2005.pdf>.
- (5) Hunley, J. D. The History of Solid-Propellant Rocketry: What we do and do not know; American Institute of Aeronautics and Astronautics, Presented as an Invited Paper at the 35th AIAA, ASME, SAE, ASEE Joint Propulsion Conference and Exhibit, 1999.
- (6) Colvin, V. L. The potential environmental impact of engineered nanomaterials. *Nat. Biotechnol.* **2003**, *21* (10), 1166–1170.
- (7) Foley, S.; Crowley, C.; Smahih, M.; Bonfils, C.; Erlanger, B. F.; Seta, P.; Larroque, C. Cellular localisation of a water-soluble fullerene derivative. *Biochem. Biophys. Res. Commun.* **2002**, *294* (1), 116–119.
- (8) Lundborg, M.; Johard, U.; Lastbom, L.; Gerde, P.; Camner, P. Human alveolar macrophage phagocytic function is impaired by aggregates of ultrafine carbon particles. *Environ. Res.* **2001**, *86* (3), 244–253.
- (9) Renwick, L. C.; Donaldson, K.; Clouter, A. Impairment of alveolar macrophage phagocytosis by ultrafine particles. *Toxicol. Appl. Pharmacol.* **2001**, *172* (2), 119–127.
- (10) Guang, J.; Wang, H.; Yan, L.; Wang, X.; Pei, R.; Yan, T.; Zhao, Y.; Guo, X. Cytotoxicity of Carbon Nanomaterials: Single-Wall Nanotube, Multi-Wall Nanotube, and Fullerene. *Environ. Sci. Technol.* **2005**, *39* (5), 1378–1383.
- (11) Braydich-Stolle, L.; Hussain, S.; Schlager, J. J.; Hofmann, M. C. In vitro cytotoxicity of nanoparticles in mammalian germline stem cells. *Toxicol. Sci.* **2005**, *88* (2), 412–419.
- (12) Kleinman, M. T.; Sioutas, C.; Chang, M. C.; Boere, A. J.; Cassee, F. R. Ambient fine and coarse particle suppression of alveolar macrophage functions. *Toxicol. Lett.* **2003**, *137* (3), 151–158.
- (13) Skebo, J. E.; Grabinski, C. M.; Schrand, A. M.; Schlager, J. J.; Hussain, S. M. Assessment of Metal Nanoparticle Agglomeration, Uptake, and Interaction Using High Illuminating System. *Int. J. Toxicol.* **2007**, *26* (2), 151–158.
- (14) Carmichael, J.; DeGraff, W. G.; Gazdar, A. F.; Minna, J. D.; Mitchell, J. B. Evaluation of a tetrazolium-based semiautomated colorimetric assay: assessment of chemosensitivity testing. *Cancer Res.* **1987**, *47* (4), 936–942.
- (15) Paine, R., III.; Morris, S. B.; Jin, H.; Wilcoxon, S. E.; Phare, S. M.; Moore, B. B.; Coffey, M. J.; Toews, G. B. Impaired functional activity of alveolar macrophages from GM-CSF-deficient mice. *Am. J. Physiol Lung Cell Mol. Physiol.* **2001**, *281* (5), L1210–L1218.
- (16) Powers, K. W.; Brown, S. C.; Krishna, V. B.; Wasdo, S. C.; Moudgil, B. M.; Roberts, S. M. Research strategies for safety evaluation of nanomaterials. Part VI. Characterization of nanoscale particles for toxicological evaluation. *Toxicol. Sci.* **2006**, *90* (2), 296–303.